Polymer Journal (2019) 51:1189–1195
https://doi.org/10.1038/s41428-019-0238-8

ORIGINAL ARTICLE

Reinforcement of polyamide 6/66 with a 9,9′-bis(aryl)fluorene-modified cellulose nanofiber

Masayuki Sugimoto[1,2] · Masahiro Yamada[1] · Hirokazu Sato[2] · Katsuhisa Tokumitsu[2]

Received: 30 April 2019 / Revised: 26 June 2019 / Accepted: 27 June 2019 / Published online: 30 July 2019

Abstract

We synthesized cellulose nanofiber (CNF) modified with 9,9′-bis(aryl)fluorene, which has cardo moieties (BCNF), and evaluated the properties of its polyamide 6/66 (PA) composites. As a result, it was revealed that BCNF was well dispersed in PA and had a strong reinforcing effect—even in a temperature range above the glass transition temperature—compared with unmodified CNF due to the high interface affinity between BCNF and PA.

Introduction

In recent years, the reduction of carbon dioxide emissions has become an urgent focus of efforts to prevent further global warming [1–3]. One of the approaches towards reducing emissions is lowering the weight of automobiles. Therefore, automobile companies and researchers have invested significant efforts into replacing the heavy metallic components of vehicles with light plastic materials. Polyamides in particular are widely used in this area due to their high toughness, wear resistance, and chemical resistance [4, 5]. However, many polyamides have glass transition temperatures under 100 °C; therefore, it is difficult to use them in hot areas such as those near engine components. Consequently, glass fibers have been introduced into the plastic materials to counteract these negative properties [6, 7]. However, the resulting materials also have limitations, such as high-specific gravity and rarely being recyclable.

Cellulose nanofibers (CNFs) have recently attracted significant attention and have been broadly studied as alternatives to glass or carbon fibers [8–10]. CNFs are organic fibers separated from biomass such as wood that have a unique combination of properties, including high toughness, low specific gravity, and a low coefficient of thermal expansion [11]. However, they have a large number of hydroxyl groups on their structural surface, which reduces their compatibility with plastics; therefore, improving their dispersibility through surface modification or the grafting of CNFs is an active area of research [12–14].

9,9′-bis(aryl)fluorenes that have cardo moieties in their structure have a unique symmetry and a sterically bulky structure. They have been studied as raw materials for optical plastics and as dispersants for carbon [15–18], and their high dispersibility in and compatibility with various resins have been reported [19, 20]. In addition, it has been reported that CNF modified with an aromatic ring-containing compound can effectively enhance resins [21].

In this study, we describe how the surface modification of CNFs with 9,9′-bis(aryl)fluorene can improve their dispersibility in polyamides and reinforce the interface between CNF and polyamides, particularly in high-temperature regions.

Materials and methods

Materials

CNF (CELISH KY-100N) and polyamide 6/66 (Novamid 2420J) were purchased from Daicel FineChem Ltd. (Tokyo, Japan) and DSM (Heerlen, Nederland), respectively. Bisphenol fluorene diglycidyl ether (BPFG) was obtained from Osaka Gas Chemicals (Osaka, Japan. *N,N*-Dimethylacetamide (DMAc), 1,8-diazabicyclo[5.4.0]undec-7-ene

✉ Masayuki Sugimoto
masa-sugimoto@osakagas.co.jp

[1] Energy Technology Laboratories, Osaka Gas Co., Ltd., Osaka 5540051, Japan

[2] Graduate School of Engineering, University of Shiga Prefecture, Shiga 5228533, Japan

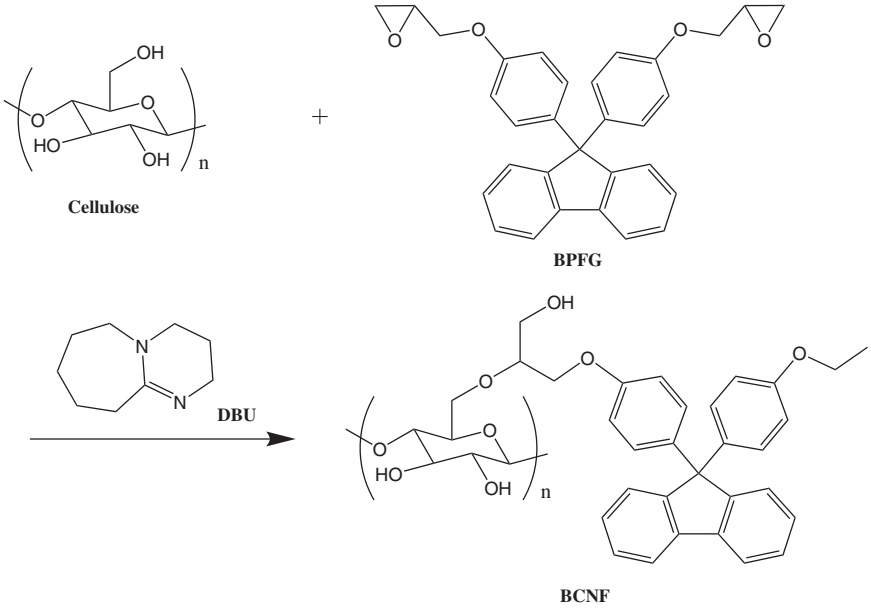

Fig. 1 Scheme showing the modification of CNF with BPFG

(DBU), and acetone were purchased from TCI (Tokyo, Japan). All materials were used without further purification.

Synthesis of fluorene-modified CNF (BCNF)

The scheme in Fig. 1 shows the synthesis of the fluorene-modified CNF (BCNF). CNF (9.7 g solid content, 15% aqueous dispersion) and 206 g of DMAc were added to a 1000 mL round-bottomed flask and stirred at ambient temperature until a homogeneous mixture was formed. The mixture was evaporated at 70 °C until the water content was lower than 1.0%. A further 498 g of DMAc, 9.7 g of BPFG, and 1.95 g of DBU (as a catalyst) were then added and the mixture was heated at 125 °C for 6 h under an atmosphere of nitrogen. The reaction solution was washed with 500 g of acetone three times to remove unmodified BPFG and catalyst. The modification ratio of the obtained BCNF was determined by Fourier transform infrared spectroscopy (FT-IR). The morphology of CNF before and after the reaction was observed using scanning electron microscopy (SEM).

Preparation of polyamide/CNF composites and films

Prior to extrusion, PA was dried in an oven for 5 h at 80 °C under vacuum. Initially, the PA was added to a kneader (Labo-Plastmill 50M, TOYOSEIKI) at 220 °C and kneaded for 2 min at 20 rpm and then CNF or BCNF was added to the kneader at 220 °C, at which no thermal decomposition was found to occur according to TG/DTA analysis, and kneading was continued for 6 min at 50 rpm. CNF and BCNF were used in the hydrated state because it is difficult to remove remaining water from CNF nanofiber structures. CNFw, BCNFw, and BCNFa denote CNF in water (15%), BCNF in water (16%), and BCNF in acetone (20%), respectively. Table 1 shows the compositions of the PA and CNF/BCNF composites; the values given for CNF/BCNF are the weights as a solid excluding the water and acetone content of CNF/BCNF means as a solid. The obtained mixture was crushed using a cutter mill.

Characterization of the CNF dispersion state

The dispersion state of PA/CNF-5 and PA/BCNFa-5 were studied by transmission electron microscopy (TEM). The test films for TEM analysis were prepared by microtome. The thickness of the film was 100 nm and the acceleration voltage was 100 kV.

DMA analysis of composites

The molecular dynamics properties of the composites were studied with a dynamic mechanical analyzer (DMA) using tension mode. The test films for DMA analysis were prepared by press molding. The effective size of the films was $3 \times 30\ \mathrm{mm}^2$ and the thickness was 0.3 mm. The films were vibrated with a dual-cantilever fixture at 1, 2, 4, 8, 16, 32, 64, and 128 Hz. All subsequent tests were conducted from −150 to 200 °C at 2 °C/min with a strain of 0.015%. The activation energy (E_a) at the glass transition temperature was calculated to evaluate the binding force of CNF and BCNF on the matrix using Müller and Huff's equation [22]

$$\ln(\mathrm{f}) = -\frac{E_a}{RT} + \frac{\Delta S}{R}$$

where f, E_a, R, T, and ΔS are frequency [Hz], activation energy [J mol^{-1}], gas constant [J K^{-1} mol^{-1}], glass

Table 1 Composition of PA and CNF BCNF composites

Sample code	Material and content (wt%)			
	PA 6/66	CNFw	BCNFw	BCNFa
PA	100	0	0	0
PA/CNF-5	95	5	0	0
PA/CNF-10	90	10	0	0
PA/CNF-20	80	20	0	0
PA/BCNFw-10	90	0	10	0
PA/BCNFw-20	80	0	20	0
PA/BCNFa-5	95	0	0	5
PA/BCNFa-10	90	0	0	10
PA/BCNFa-20	80	0	0	20

transition temperature of PA [K], and entropy change [J K^{-1} mol^{-1}], respectively.

Tensile tests of composites over a high-temperature range

To evaluate the mechanical properties of the composites over a high-temperature range, tensile tests were conducted using the same DMA at 100 and 150 °C. The size of the film for the test was 3×30 mm^2 and the thickness was 0.3 mm. The tensile tests were performed with a tension rate of 0.0175 mm/s after the sample chamber was held at each temperature for 5 min to stabilize the temperature.

Thermal–mechanical analysis of composites

To evaluate the coefficient of linear thermal expansion (CTE), thermomechanical analysis (TMA) was conducted using a Thermo Plus2 TMA 8310. The size of the specimen was $24 \times 5 \times 0.3$ mm^3. The measurement was performed using tension mode from 40 to 190 °C at 5 °C/min with a static loading of 49 mN. A constant N_2 flow rate of 200 mL/min was maintained through the TMA instrument during the measurement to prevent oxidation.

Results and discussion

Characterization of BCNF

A scheme outlining BCNF synthesis is shown in Fig. 1. Cellulose has a highly reactive primary alcohol hydroxyl group at the C6-position of a glucose unit. Therefore, the epoxy group of BPFG preferentially attacked the hydroxyl group at the C6-position of cellulose and formed ether bonds. The results of the high-performance liquid chromatography measurements showed that most of the epoxy groups had been opened and formed two hydroxyl groups; however, some of them may have caused a crosslinking reaction or remained as an epoxy group. Figure 2a, b are SEM images of before and after the CNF modification reaction, respectively. No CNF aggregation was observed before or after the modification reaction. The modification rate by BPFG was evaluated by FT-IR using a standard curve method. The aromatic ring deformation at 1506 cm^{-1} was characteristic of fluorene aromatic rings and the modification rate, calculated using the same method as in a previous study, was DS = 0.048 [23].

Morphological analysis of composites

The dispersion state and interface between PA and CNF/BCNF were investigated using TEM. Figure 3a–d show the TEM images obtained for the PA/CNF-5 and PA/BCNFa-5 composite films, respectively. Compared with PA/BCNF, larger aggregated particles of CNF and larger interfacial voids between PA and CNF were observed in PA/CNF. This shows that homogeneous dispersion of CNF and interfacial reinforcement between PA and CNF were achieved by modification of the CNF surface with BPFG.

Mechanical properties and molecular dynamics of composites

The storage moduli (E') of the composites in the temperature range of 0–200 °C are shown in Fig. 4. The E' of the PA/CNF, PA/BCNFw, and PA/BCNFa increased in accordance with the content of CNF or BCNF in PA across the whole temperature range, and the E' of PA/BCNFw and PA/BCNFa were found to be higher than that of PA/CNF with a similar fiber content. This tendency is particularly notable above the glass transition temperature. For example, the E' value at 100 °C, which is above the glass transition temperature, increased from 244 MPa for neat PA to 372 MPa for PA/CNF-10, 668 MPa for PA/BCNFw-10, and 824 MPa for PA/BCNFa-10. It can be concluded that modification of BPFG is effective because addition of 5% acetylated CNF to polyamide 4.10 did not significantly improve the E' value at the same condition of 50 rpm kneading in ref. [14]. In addition, the E' of PA/BCNFa was higher than that of PA/BCNFw, particularly in the high-temperature range. This observation is attributed to the difference in polarity between acetone and water. We therefore focused on PA/CNF and PA/BCNFa. The loss tangent ($\tan \delta$) of the composite is shown in Fig. 5. The peaks at ~60 °C were assigned to the α relaxation (glass transition) of PA. Because the peak square of $\tan \delta$ shows the strength of the molecular motion of the polymer, we compared the square ratio of neat PA and CNF or BCNF composites as shown in Table 2. The findings indicate that

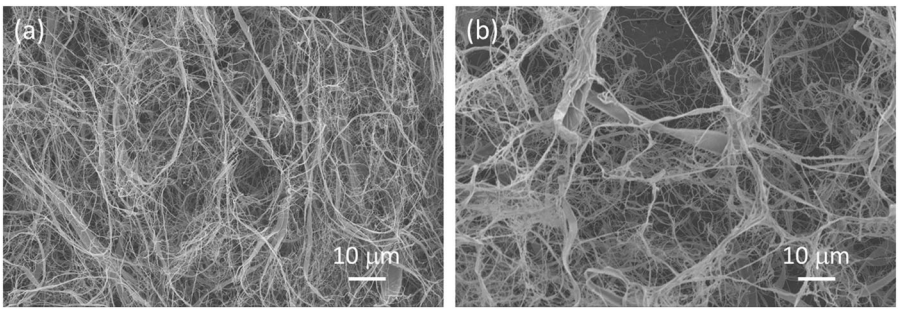

Fig. 2 SEM images of cellulose nanofibers (**a**) before and (**b**) after BPFG modification

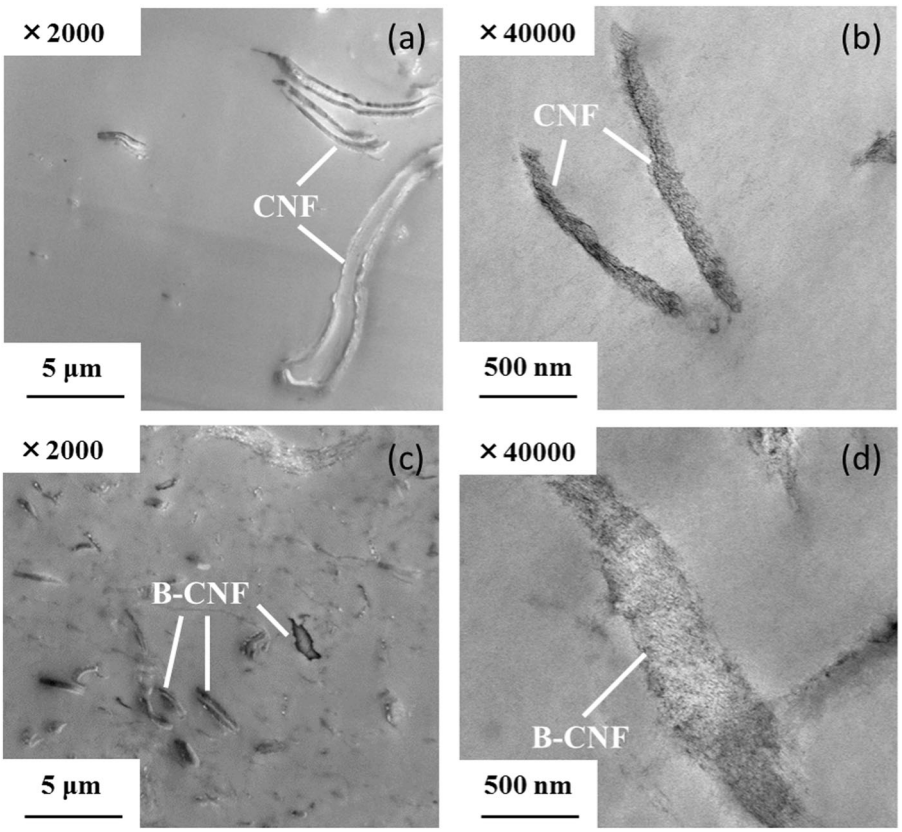

Fig. 3 TEM images of PA/CNF (**a**, **b**) and PA/BCNFa-5 (**c**, **d**)

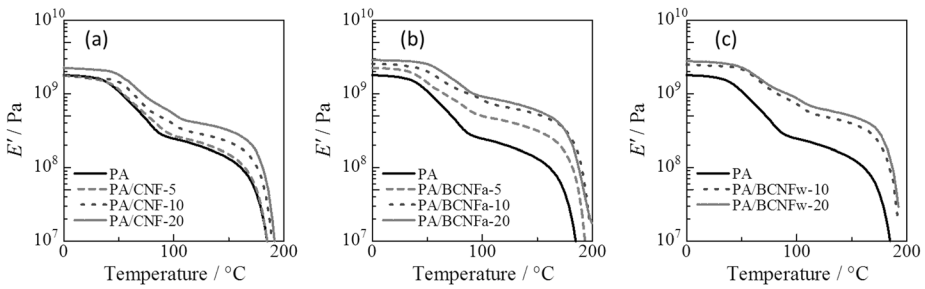

Fig. 4 Storage moduli of (**a**) PA/CNF and (**b**) PA/BCNFa

the tan δ values of PA/CNF and PA/BCNFa were lower than that of neat PA and this observation is particularly stark for BCNF versus CNF. These results suggest that the molecular motion of PA was restricted by the presence of CNF and BCNF, and the interaction between PA and BCNF is much stronger than that of PA/CNF.

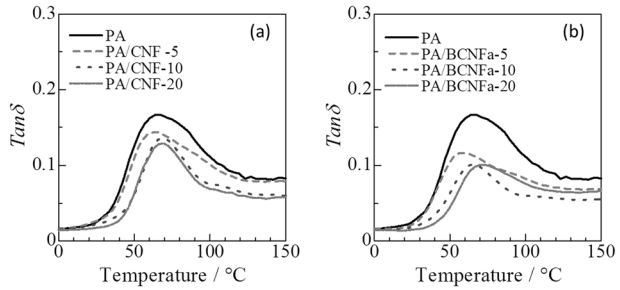

Fig. 5 tan δ of (**a**) PA/CNF and (**b**) PA/BCNFa

Table 2 tan δ ratio of PA/CNF and PA/BCNFa to neat PA

Sample code	CNF/BCNF content (wt%)			
	0	5	10	20
PA/CNF/-	1	0.75	0.62	0.58
PA/BCNF/-		0.65	0.46	0.47

Table 3 Activation energy (E_a) of the principal PA chain

Sample code	CNF/BCNF content (wt%)			
	0	5	10	20
E_a of PA/CNF (kJ mol^{-1})	152	162	209	236
E_a of PA/BCNFa (kJ mol^{-1})		217	231	318

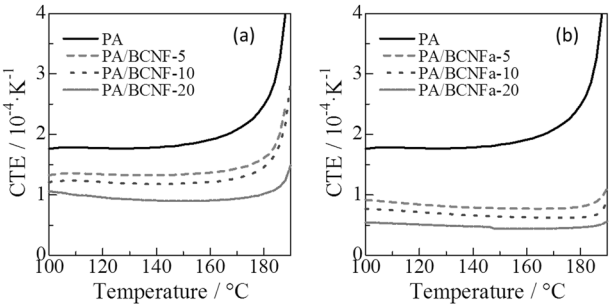

Fig. 6 CTE of (**a**) PA/CNF and (**b**) PA/BCNFa

Further, to evaluate the molecular motion of the PA chain, the activation energy (E_a) of the PA principal chain was calculated for the different CNF/BCNF contents using Müller and Huff's equation, as shown in Table 3. The results show that the addition of both PA/CNF and PA/BCNFa caused the E_a of the PA principal chain to increase with increasing CNF or BCNF content. This increased E_a also suggests restriction of the PA principal chain and its molecular motion as a result of CNF and BCNF addition. Because the increase of E_a is larger in PA/BCNF than PA/CNF, BPFG modification is thought to increase the interaction between CNF and PA.

Thermal properties of composites

Figure 6 shows the CTE of PA/CNF and PA/BCNF above 100 °C. The value of CTE was calculated from the slope of the TMA results separated every 2 °C. There was little change with increasing temperature near the melting point of PA (193 °C) observed for the PA/CNF composites and there was no dependence on the amount of CNF. In contrast, for PA/BCNF, the observed changes were shifted to higher temperatures by increasing BCNF. The CTE of both PA/CNF and PA/BCNF above 100 °C decreased in accordance with the content of CNF or BCNF in the PA, and the CTE of PA/BCNF was consistently smaller than that of PA/CNF with a similar content. The CTE at 150 °C decreased from $1.83 \times 10^{-4}\,K^{-1}$ for near PA to $1.19 \times 10^{-4}\,K^{-1}$ for PA/CNF-10 and $0.64 \times 10^{-4}\,K^{-1}$ for PA/BCNFa-10. This result indicates that the CNF modified with BPFG can interact with PA more strongly than unmodified CNF.

Evaluation of the mixture state of the composites using the insoluble composite mixture model

From the DMA and TMA results, the volume fractions of the PA phase interacting with CNF and BCNF were estimated by means of the mixture rule for an incompatible system, as shown by the following equation [23]:

$$\alpha_c = (1-\varphi)\alpha_a + \varphi\frac{\alpha_A(1-\lambda)E_A + \alpha_B\lambda E_B}{(1-\lambda)E_A + \lambda E_B}$$

where α_A, α_B, and α_C are the CTE [K^{-1}] of components A, B, and the composite of A and B; E_A and E_B are the modulus [Pa] of A and B; φ is the volume fraction of A (A′) interacting with B; and λ represents the volume fraction of B when φ is taken as a whole. In this study, fitting was performed assuming A as independent of PA, A′ as PA interacting with CNF or BCNF, and B as CNF or BCNF. The CTE of $\alpha_B = 0.17$ ppm K^{-1} and the modulus of $E_B =$ 138 GPa are used as constant values in the measurement temperature range [11]. In addition, because the modification rate of BCNF is sufficiently small (DS = 0.048), the same value for CNF was used assuming that the cardo material does not affect the physical properties of CNF. The results in Fig. 7 show that for PA/CNF, the volume fraction of PA not interacting with CNF decreased as the amount of added CNF increased and that PA/CNF showed a linear decrease at added amounts above 5 wt%. In contrast, it was found that the volume fraction of PA not interacting with BCNF significantly decreased at 5 wt% of PA/BCNF and thereafter gently decreased. Because PA/BCNF is not linearly related to the increase in the added amount of

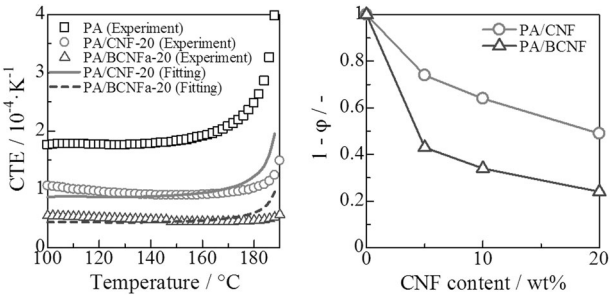

Fig. 7 Fitting results of (**a**) CTE and (**b**) $1-\varphi$

BCNF, the reduction in the amount of PA component not interacting with BCNF is considered to result from aggregation in the high added fiber range. Modifying CNF with BPFG improves the interaction between PA and CNF and increases the degree of restraint of PA molecular chains by CNF; therefore, the strength of the interface between PA and CNF is found to be improved.

Conclusion

In this study, we successfully synthesized CNF modified with BPFG and evaluated the properties of its composites with PA. BPFG modification of CNF markedly improved the physical properties of PA, including E' and the CTE, especially under high-temperature conditions. These improvements are attributed to the following factors:

1. Improvement of CNF dispersion in PA by modification of BPFG derived from the bulky structure of BPFG (inhibition of hydrogen bond formation between fibers during kneading).
2. Improvement of the interface interaction between BCNF and PA by surface hydrophobization of CNF.

For these reasons, it is concluded that modifying CNF with a fluorene derivative possessing cardo moieties is a promising approach for reinforcing polyamide resin with CNF.

Acknowledgements We thank Sarah Dodds, Ph.D., from the Edanz Group (www.edanzediting.com/ac) for editing a draft of this manuscript.

Compliance with ethical standards

Conflict of interest The authors declare that they have no conflict of interest.

References

1. Le Quéré C, Andres RJ, Boden T, Conway T, Houghton RA, House JI, et al. The global carbon budget 1959–2011. Earth Syst Sci Data. 2013;5:165–85.
2. Smith Pete, Davis Steven J, Creutzig Felix, Fuss Sabine, Minx Jan, Gabrielle Benoit, et al. Biophysical and economic limits to negative CO_2 emissions. Nat Clim Change. 2016;6:42–50.
3. Rogelj Joeri, Elzen Michelden, Höhne Niklas, Fransen Taryn, Fekete Hanna, Winkler Harald, et al. Paris Agreement climate proposals need a boost to keep warming well below 2 °C. Nature. 2016;534:631–9.
4. Levchik SV, Weil ED, Lewin M. Thermal decomposition of aliphatic nylons. Polym Int. 1999;48:532–3.
5. Wang W-Z, Zhang Y-H. Environment-friendly synthesis of long chain semiaromatic polyamides. eXPRESS Polym Lett. 2009;3:470–6.
6. Mouhmida B, Imada A, Benseddiqa N, Benmedakhe'neb S, Maazouzc A. A study of the mechanical behaviour of a glass fibre reinforced polyamide 6, 6: experimental investigation. Polym Test. 2006;25:544–52.
7. Davim JPaulo, Silva LeonardoR, António Festas, Abrão AM. Machinability study on precision turning of PA66 polyamide with and without glass fiber reinforcing. Mater Des. 2009;30:228–34.
8. Eichhorn SJ, Dufresne A, Aranguren M, Marcovich NE, Capadona JR, Rowan SJ, et al. Review: current international research into cellulose nanofibers and nanocomposites. J Mater Sci. 2010;45:1–33.
9. Isogai Akira, Saito Tsuguyuki, Fukuzumi Hayaka. TEMPO-oxidized cellulose nanofibers. Nanoscale. 2011;3:71–85.
10. Orts WilliamJ, Shey Justin, Imam SyedH, Glenn GregoryM, Guttman MaraE, Revol Jean-Francois. Application of cellulose microfibrils in polymer nanocomposites. J Polym Environ. 2005;13:301–6.
11. Nishino Takashi, Matsuda Ikuyo, Hirao Koichi. All-cellulose composite. Macromolecules. 2004;37:7683–7.
12. Sato Akihiro, Kabusaki Daisuke, Okumura Hiroaki, Nakatani Takeshi, Nakatsubo Fumiaki, Yano Hiroyuki. Surface modification of cellulose nanofibers with alkenyl succinic anhydride for high-density polyethylene reinforcement. Compos: Part A. 2016;83:72–9.
13. Enomoto-Rogers Yukiko, Kamitakahara Hiroshi, Takano Toshiyuki, Nakatsubo Fumiaki. Cellulosic graft copolymer: poly (methyl methacrylate) with cellulose side chains. Biomacromolecules. 2009;10:2110–7.
14. Leszczyn´ska Agnieszka, Kicilin´ski Paweł, Pielichowski Krzysztof. Biocomposites of polyamide 4.10 and surface modified microfibrillated cellulose (MFC): influence of processing parameters on structure and thermomechanical properties. Cellulose. 2015;22:2551–69.
15. Kawasaki Shinichi, Yamada Masahiro, Kobori Kana, Jin Fengzhe, Kondo Yoshikazu, Hayashi Hideki, et al. Synthesis and chemical, physical, and optical properties of 9,9-diarylfluorene-based poly (ether-ether-ketone). Macromolecules. 2007;40:5284–9.
16. Kazamaa S, Teramoto T, Haraya K. Carbon dioxide and nitrogen transport properties of bis(phenyl)fluorene-based cardo polymer membranes. J Membr Sci. 2002;207:91–104.
17. Kawasaki Shinichi, Yamada Masahiro, Kobori Kana, Jin Fengzhe, Takata Toshikazu. Fine dispersion of carbon black in fluorene-based resin. Polym Compos. 2008;29:1044–8.
18. Liou Guey-Sheng, Yen Hung-Ju, Su Yi-Ting, Lin Hung-Yi. Synthesis and properties of wholly aromatic polymers bearing cardo fluorene moieties. J Polym Sci: Part A. 2007;45:4352–63.
19. Tokumitsu Katsuhisa, Matsuura Takuya, Kawasaki Shinichi, Tashiro Kohji. A study on crystallization behavior for poly (lactic

acid) in addition of cardo materials. J Soc Mater Sci Jpn. 2015;64:1–6.
20. Kawasaki Shinichi, Yamada Masahiro, Kobori Kana, Sakamoto Hiroki, Kondo Yoshikazu, Jin Fengzhe, et al. Preparation of a novel alloy composed of fluorene-based polyester and polycarbonate and their properties for the optical uses. J Appl Polym Sci. 2009;111:461–8.
21. Nanocellulose Symposium 2013. http://www.rish.kyoto-u.ac.jp/labm/wp-content/uploads/2013/04/cellulosesymposium2013.pdf. Accessed 20 Apr 2019.
22. Müller H, Hoff K. Zur Frage der reduzierten Darstellung des dielektrischen Spektrums bei Hochpolymeren. Kolloid-Z. 1959;166:44.
23. Terakura Kosuke, Tokumitsu Katsuhisa, Yamada Masahiro, Sugimoto Masayuki. Mechanical and thermal properties of poly (lactic acid) with cellulose nanofiber modified by bisphenol fluorene diglycidyl ether (BPFG). Nihon Reoroji Gakkaishi. 2016;44:39–45.